

Probing R -parity violation in the production of $tc(ct)$ on the lepton colliders

Yu Zeng-Hui^{a,c} Herbert Pietschmann^a Ma Wen-Gan^{b,c} Han Liang^c Jiang Yi^c

^aInstitut für Theoretische Physik, Universität Wien, A-1090 Vienna, Austria

^bCCAST (World Laboratory), P.O. Box 8730, Beijing 100080, P.R. China

^cDepartment of Modern Physics, University of Science and Technology of China (USTC), Hefei, Anhui 230027, P.R. China

ABSTRACT

We studied the process $e^+e^- \rightarrow tc + ct$ in a R_p violating supersymmetric model with effects from both B - and L -violating interactions. The calculation shows that it is possible to either detect the R_p violating signal at the Next Linear Collider or get more stringent constraints on the heavy-flavor R_p couplings. A comparison with results from $e^+e^- \rightarrow tc + ct$ may allow to distinguish between B - and L -violating interactions. For very clean background conditions and R_p violation parameters close to present limits, a future detection of B -violating interactions should be possible. The process of $e^+e^- \rightarrow tc + ct$ is also considered.

PACS number(s): 13.65.+i, 13.88.+e, 14.65.-q, 14.80.Dg, 14.80.Gt

Supported in part by Committee of National Natural Science Foundation of China and Project IV.B.12 of scientific and technological cooperation agreement between China and Austria

I. Introduction

In the minimal supersymmetric model (MSSM) [1], R-parity symmetry (R_p) is imposed on the superfield to guarantee the B- and L-conservation automatically. This symmetry is defined by

$$R = (-1)^{3B + L + 2S} \quad (1)$$

where S is the spin of the particle. The discrete symmetry was introduced [2] to avoid catastrophic proton decays from R_p -violating interactions. In the models of R_p -conservation, superparticles can be only pair produced and the lightest superparticle (LSP) will be stable. Thus the LSP is a candidate of cold dark matter in the universe.

However, in order to avoid proton decays we just need either B-conservation or L-conservation [3]. Moreover, models of R_p violation provide for neutrino masses and mixing. In those models neutrinos may get tree-level mass contributions via mixing with gauginos and higgsinos, and of course also from one-loop corrections. Unlike the general see-saw mechanism, which involves a high energy scale (about $10^{12} - 10^{16}$ GeV), we can explain neutrino masses with weak-scale physics. With first signals for neutrino oscillations from atmospheric neutrinos observed in Super-Kamiokande [4], R_p is getting more and more interesting.

Possible signals of R_p -violation in collider experiments have also been discussed. In the HERA e^+p deep inelastic scattering (DIS) [5], an anomaly has been observed. It was found that the rate of Neutral Current (NC) events is higher than that predicted by the Standard Model when Q^2 is larger than $15,000 \text{ GeV}^2$ (The possibility of a statistical uc-

tuation is about 10^{-3}). For Charge Current(CC) events, a difference between observation and prediction of SM also exists, although not as large as for NC events. The anomaly can be explained beautifully by R_p supersymmetric mechanism, providing a possible hint for R-parity violation.

Because R_p models open many channels forbidden or highly suppressed in R_p conserving models, we can get many constraints from low-energy phenomenology [6]. Results are collected in Ref.[7].

Let us now consider lepton colliders. Possible ways to find a signal of R_p are as follows:

1. Single production of sparticles and LSP decay.(direct signal)
2. Fermion pair productions are different in R_p models and R_p conservation models.(indirect signal)

3 Flavor Changing Neutral Current (FCNC) and CP violation.(indirect signal)

In this paper we will concentrate on the third way. Process $l^+ l^- \rightarrow f_j f_{j^0}$ (J and J^0 are different flavors) is calculated from the L-violation terms of R_p models[8].

Although many constraints from low-energy phenomenology were already given, R_p parameters involving heavy flavors are not limited strongly. With the assumption of family symmetry [9], we can get $\lambda_{ijk} = Y_{ijk}$ (where λ_{ijk} are defined in Eq.(2.1) and Y_{ijk} are Yukawa couplings). So it is still possible to detect them on future colliders in the high energy region.

In this paper we will use $t\bar{t}$ production to probe R_p signals on the Next-Linear Collider (NLC), First-Muon-Collider(FMC) [10] and possibly also at LEP2. Compared

with LEP2, NLC will have much higher luminosity and energy, providing a powerful probe. This is even more true should the FCC go into operation.

Although many processes with L-violation on lepton colliders have been calculated, B-violation effects are rarely considered. Up to now B-violation parameters involving heavy flavors are still constrained weakly. For example ϵ_{2ij}'' and ϵ_{3ij}'' , get their strongest constraints from the width ratio of Z to leptons and hadrons, still being order of 10^{-1} . Hence future colliders can either detect them (if they are close to present upper limits) or strongly improve the limits.

Let us consider the possible background:

1. Standard Model.

The background from SM is suppressed by the GIM mechanism. The process of $e^+e^- \rightarrow t\bar{c}(c\bar{t})$ was considered by C.S.Huang et al[11]. They pointed out that the cross section of the process is about 10^{-9} fb for cm energy of about 200-500 GeV, thus being a negligible background for R_p effects.

2. Two-Higgs-Doublet-Model (THDM).

In the so called Model III of Ref.[12], which gives the strongest effects of FCNC, the process $e^+e^- \rightarrow t\bar{c}$ was considered by Atwood et al[12] and $e^+e^- \rightarrow t\bar{c}(c\bar{t})$ by Y.Jiang et al[12]. The results show that there would be 0.1 events for $e^+e^- \rightarrow t\bar{c}(c\bar{t})$ and several events for $e^+e^- \rightarrow t\bar{c}$ for luminosity about 50fb^{-1} . Because the effects depended on the resonance of higgses, it will be easy to distinguish them from effects from R_p violation.

3. MSSM with R_p conservation.

Squark mixing can generate FCNC in this model. But under the assumption of alignment of $S D$ inopoulos[13], it should be very small mixing between up-type squarks can be as small as 10^{-3} to 10^{-5} times the KM matrix elements.

In Left-Right Symmetric Models there is also a contribution to FCNC from Z^0 decay. Because the mass of Z^0 is very large, we can omit it in our calculations, where the center of mass energy is less than 500 GeV.

After the general observation concerning the process $l^+ l^- \rightarrow t c + c t$, we define the supersymmetric \mathcal{R}_p interaction in section 2. In section 3 we give the analytical calculations of $e^+ e^- \rightarrow t c + c t$. In section 4 the numerical results of the processes $e^+ e^- \rightarrow t c + c t$ and $\mu^+ \mu^- \rightarrow t c + c t$ are presented. The conclusion is given in section 5 and some details of the expressions are listed in the appendix.

II. R-parity violation (\mathcal{R}_p) in MSSM

All renormalizable supersymmetric \mathcal{R}_p interactions can be introduced in the superpotential[6]:

$$W_{\mathcal{R}_p} = \frac{1}{2} \epsilon_{ijk} L_i \tilde{L}_j E_k + \epsilon_{ijk} L_i \tilde{Q}_j D_k + \frac{1}{2} \epsilon_{ijk} U_i \tilde{D}_j D_k + \epsilon_{ijk} L_i H_u : \quad (2.1)$$

where L_i , Q_i and H_u are $SU(2)$ doublets containing lepton, quark and Higgs superfields respectively, E_j (D_j , U_j) are the singlets of lepton (down-quark and up-quark), and i, j are generation indices and square brackets on them denote antisymmetry in the bracketed indices.

We ignored the last term in Eq (2.1) because its effects are rather small in our process [7][14].

So we have 9 -type, 27⁰-type and 9⁰⁰-type independent parameters left. The Lagrangian density of \mathbb{R}_p (to lowest order) is given as follows:

$$\mathcal{L}_{\mathbb{R}_p} = \mathcal{L}_{\mathbb{R}_p} + \mathcal{L}_{\mathbb{R}_p}^0 + \mathcal{L}_{\mathbb{R}_p}^{00} \quad (2.2)$$

$$\begin{aligned} \mathcal{L}_{\mathbb{R}_p} = & \sum_{[ij]k} [\tilde{\nu}_{iL} e_{kR} e_{jL} + e_{jL} e_{kR} \tilde{\nu}_{iL} + e_{kR} \tilde{\nu}_{iL}^C e_{jL} \\ & \tilde{\nu}_{jL} e_{kR} e_{iL} - e_{iL} e_{kR} \tilde{\nu}_{jL} - e_{kR} \tilde{\nu}_{jL}^C e_{iL}] + \text{h.c.} \end{aligned}$$

$$\begin{aligned} \mathcal{L}_{\mathbb{R}_p}^0 = & \sum_{ijk} [\tilde{\nu}_{iL} d_{kR} d_{jL} + \tilde{\nu}_{jL} d_{kL}^C \tilde{\nu}_{iL} + \tilde{\nu}_{kR} \tilde{\nu}_{iL}^C d_{jL} \\ & e_{iL} d_{kR} u_{jL} - \tilde{\nu}_{jL} d_{kR} e_{iL} - \tilde{\nu}_{kR} e_{iL}^C u_{jL}] + \text{h.c.} \end{aligned}$$

$$\mathcal{L}_{\mathbb{R}_p}^{00} = \sum_{i[jk]} [\tilde{\nu}_{iR} d_{kR} d_{jR}^C + \tilde{\nu}_{jR} u_{iR} d_{kR}^C + \tilde{\nu}_{kR} u_{iR} d_{jR}^C] + \text{h.c.} \quad (2.3)$$

From the interactions above, we find that only $\mathcal{L}_{\mathbb{R}_p}^0$ contributes to $l^+ l^- \rightarrow \tau^+ \tau^-$ at tree-level. So the contribution from $\mathcal{L}_{\mathbb{R}_p}$ can be neglected.

The proton lifetime limit suppresses the possibilities of both B-violation and L-violation and leads to the constraints:[7]

$$|j(\text{ or } ^0)| < 10^{-10} \left(\frac{m}{100 \text{ GeV}} \right)^2 : \quad (2.4)$$

The contributions from $L_{\cancel{p}}''$ are rather weak, but they can be separated from those of $L_{\cancel{p}}^0$. Therefore, $L_{\cancel{p}}''$ effects will be considered also.

In the past years, many limits on the parameters ϵ , ϵ^0 and ϵ'' were given from low-energy experiments. The upper limits were calculated with the assumption that only one coupling parameter is non-zero [15]. On that basis, the parameters ϵ , ϵ^0 and ϵ'' are typically less than $10^{-1} - 10^{-2} (\frac{m}{100 \text{ GeV}})^2$ [7]. Although some authors argue that the limits can be relaxed [16] if the so-called single coupling hypothesis is dropped, we shall use these upper bounds in our paper.

III. Calculations

In the following calculations we assume the parameters ϵ^0 and ϵ'' to be real. We will only consider the lowest order effects from $L_{\cancel{p}}^0$ and $L_{\cancel{p}}''$.

A. $e^+(p_3)e^-(p_4) \rightarrow t(p_1)c(p_2)$ at tree-level.

We define the Mandelstam variables as usual

$$s = (p_1 + p_2)^2 = (p_3 + p_4)^2 \quad (3a1)$$

$$t = (p_1 - p_3)^2 = (p_4 - p_2)^2 \quad (3a2)$$

$$u = (p_1 - p_4)^2 = (p_3 - p_2)^2 \quad (3a3)$$

The amplitude (as shown in Fig.1 a) is given by:

$$M = \sum_{j=1,2,3} \frac{i_{13j}^0 i_{12j}^0}{(t - m_{\text{squark}_j}^2)} u(p_1) P_R u^c(p_3) v^c(p_4) P_L v(p_2) : \quad (3a4)$$

where $P_{L,R}$ are left- and right-helicity projections respectively, $j = 1;2;3$ and the upper index c means electron-charge conjugate. The amplitude depends strongly on the products $\epsilon_{12j}^0 \epsilon_{13j}^0$ ($j = 1;2;3$).

B. Contributions from $L_{\cancel{\mu}_p}$ terms.

If we set all ϵ^0 parameters to zero, we obtain the effects of $L_{\cancel{\mu}_p}$ terms within the present upper bounds. One-loop corrections (as shown in Fig.1b) of $e^+(p_3)e^-(p_4) \rightarrow t(p_1)c(p_2)$ are proportional to the products $\epsilon_{2ij}^0 \epsilon_{3ij}^0$ ($i,j = 1;2;3$), thus it is possible to detect $\cancel{\mu}_p$ signals or get much stronger constraints on those parameters by measuring this process in future experiments.

Since the proper vertex counterterm should cancel with the counterterms of the external legs diagrams in this case, we do not have to deal with the ultraviolet divergence. Thus we simply take the sum of all (unrenormalized) reducible and irreducible diagrams and the result is finite and gauge invariant. In the Appendix we will give the details of the amplitudes.

C. Total cross sections

In a similar way we obtain the amplitude for process $e^+e^- \rightarrow ct$. Thus the total cross section for the process $e^+e^- \rightarrow ct + \bar{c}t$ is:

$$\sigma(s) = \frac{2N_c}{16s^2} \sum_{\epsilon}^Z \int_{\epsilon}^X d\epsilon \sum_{\text{spins}} |M|^2; \quad (3.5)$$

where M is the amplitude and $\hat{t} = \frac{1}{2} (m_t^2 + m_c^2 - s) \pm \sqrt{s^2 + m_t^4 + m_c^4 - 2sm_t^2 - 2sm_c^2 - 2m_t^2m_c^2}$.

Here we have neglected the masses of electron and muon. $N_c = 3$ is the colour factor and the bar over summation means averaging over initial spins.

Similarly we obtain the total cross section of $e^+e^- \rightarrow tc + ct$. Assuming values for all input parameters, we obtain numerical results.

IV. Numerical results

In the numerical calculations we assume $m_{\tilde{q}} = m_{\tilde{t}}$ and consider the effects from $L_{\tilde{q}\tilde{q}}^0$ and $L_{\tilde{q}\tilde{p}}^0$ separately. For the B-violating parameter $\tilde{a}_{2ij} \tilde{a}_{3ij}$ ($i, j = 1, 2, 3$), the upper bounds of \tilde{a}_{223} and \tilde{a}_{323} dominate all other parameters. Thus we neglect all other \tilde{a} terms. For the L-violating parameters we set $\tilde{a}_{12j}^0 = \tilde{a}_{13j}^0 = 0.1$ ($j = 1, 2, 3$) when $m_{\tilde{q}} = 100$ GeV, which agrees with the product coupling limits also. For the e^+e^- colliders, the parameters \tilde{a}_{22j}^0 and \tilde{a}_{23j}^0 can be larger because they involve heavier flavor. In this case we use the data of reference [6].

In Fig 2, we show the cross section of $e^+e^- \rightarrow tc + ct$ as function of cm. energy of the electron-positron system at the upper bounds of \tilde{a} , i.e. $\tilde{a}_{12j}^0 \tilde{a}_{13j}^0 = 0.01$. We take $m_{\tilde{t}} = m_{\tilde{q}} = 100$ GeV (solid line) and $m_{\tilde{t}} = m_{\tilde{q}} = 150$ GeV (dashed line), respectively. There we take same coupling parameters for different $m_{\tilde{q}}$ for comparing the effects of mass of squarks in the process. The results show that the cross sections can be 0.02 pb for solid line and 0.006 pb for dashed line at $\sqrt{s} = 190$ GeV, which is the present LEP running energy. So if the electron-positron integrated luminosity is 150 pb^{-1} [7], we can expect about 3 events when $m_{\tilde{t}} = m_{\tilde{q}} = 100$ GeV. At $\sqrt{s} = 200$ GeV and luminosity about 200 pb^{-1} , we expect 8 events from our results. Even if this sounds too optimistic, it may be worthwhile to consider this process once the LEP energy is above the threshold of

single top-quark production. For the NLC, with cm energy about 500 GeV and luminosity about 50 fb^{-1} , thousands of events should be observed at the present upper bounds of the parameters.

In Fig.3, we plot the cross section of $e^+e^- \rightarrow tc + ct$ as function of cm energy of the e^+e^- system with the upper bounds of θ , i.e. $\theta_{22j}^0 = 0.18$ and $\theta_{23j}^0 = 0.36$ (see Ref.[6]). We take again $m_t = m_q = 100 \text{ GeV}$ for the solid line and $m_t = m_q = 150 \text{ GeV}$ for the dashed line. The cross sections are much larger than those of Fig.2. That is because from present data the upper limits of θ_{22j}^0 and θ_{23j}^0 are larger than those of θ_{12j}^0 and θ_{13j}^0 . The cross section can be about 1 pb when $\sqrt{s} = 200 \text{ GeV}$, which means we can get hundreds of events at colliders with the same luminosity as LEP, if the coupling parameters are close to present upper limits.

In order to give more stringent constraints for θ in future experiments, we draw the effects from possible B-violating terms in Fig.4, where the cross section of $e^+e^- \rightarrow tc + ct$ as function of cm energy is given. (The solid line is for $m_t = m_q = 100 \text{ GeV}$ and dashed-line for $m_t = m_q = 150 \text{ GeV}$). When $\theta_{223}'' \theta_{323}''$ is about 0.625 (see Ref.[6]), the cross section will be about 0.5 fb at $\sqrt{s} = 200 \text{ GeV}$ or 0.9fb at $\sqrt{s} = 500 \text{ GeV}$. That corresponds to 0.1 event at LEP or 45 events at the NLC.

Let us compare the results with those from $e^+e^- \rightarrow tc + ct$ of reference [17]. It turns out that B-violating terms (i.e. $L_{\cancel{q}p}''$) give similar effects in both processes, whereas L-violation (i.e. $L_{\cancel{q}p}^0$) contributes much less in $tc + ct$ collisions than in e^+e^- processes. Therefore, a combination of the results of both these processes allows for a determination of the

source for R_p -violation (i.e. either from L -violation or from B -violation)

IV. Conclusion

We studied the processes $e^+e^- \rightarrow tc + ct$ and $\mu^+\mu^- \rightarrow tc + ct$ in a supersymmetric model with explicit R_p -violation. The calculations show that it is possible to test the model at future LEP and the future NLC experiments, provided the couplings (\tilde{g} -type) are large enough within the present experimentally admitted range. We can even detect possible B -violating terms in future lepton colliders with higher energy and higher luminosity than LEP. We also considered the possibility of production of tc and ct at $\mu^+\mu^-$ colliders. The results show that these colliders may allow to test R_p violation.

The authors would like to thank Prof. H. Stremnitzer for reading the manuscript.

Appendix

A. Loop integrals:

We adopt the definitions of two- and three-one-loop Passarino-Veltman integral functions in reference [18][19]. The integral functions are defined as

1. The two-point integrals are:

$$fB_0; B_1; B_2; g(p; m_1; m_2) = \frac{(2\pi)^{4-n}}{i^2} \int d^n q \frac{f_1(q); q \cdot q; g}{[q^2 - m_1^2][(q+p)^2 - m_2^2]}; \quad (A.1)$$

The function B_0 should be proportional to p^2 :

$$B_0(p; m_1; m_2) = p^2 B_1(p; m_1; m_2) \quad (A.2)$$

Similarly we get:

$$B_2 = p \cdot p B_{21} + g B_{22} \quad (A.3)$$

We denote $B_0 = B_0$, $B_1 = B_1 + \frac{1}{2}$ and $B_{21} = B_{21} - \frac{1}{3}$. with $\Delta = \frac{2}{3} + \log(4)$, $\epsilon = 4 - n$. Δ is the scale parameter.

2. Three-point integrals:

$$fC_0; C_1; C_2; C_3; g(p; k; m_1; m_2; m_3) = \frac{(2\pi)^{4-n}}{i^2} \int d^n q \frac{f_1(q); q \cdot q; q \cdot q; q \cdot q; g}{[q^2 - m_1^2][(q+p)^2 - m_2^2][(q+p+k)^2 - m_3^2]}; \quad (A.4)$$

We can change it to form factors as follows:

$$C_3 = p \cdot C_{11} + k \cdot C_{12}$$

$$C_{21} = p p C_{21} + k k C_{22} + (p k + k p) C_{23} + g C_{24}$$

$$C_{31} = p p p C_{31} + k k k C_{32} + (k p p + p k p + p p k) C_{33} +$$

$$(k k p + p k k + k p k) C_{34} + (p g + p g + p g) C_{35} +$$

$$(k g + k g + k g) C_{36} \quad (A.25)$$

The numerical calculation of the vector and tensor loop integral functions can be traced back to the four scalar loop integrals A_0 , B_0 and C_0 in Ref.[12][13] and the references therein.

B. one-loop correction of the amplitude.

The amplitude of one-loop diagrams M from $L_{\cancel{P}}^{\omega}$ (Fig.1b) can be decomposed into M and M_Z terms with:

$$M = \frac{eg}{s} v(p_3) u(p_4) u(p_1) (p_1; p_2) v(p_2) \quad (A.26)$$

and

$$M_Z = \left(\frac{e}{4c_w s_w} \right) \frac{g}{s} \frac{k k = m_Z^2}{m_Z^2} v(p_3) ((2 - 4s_w^2) P_L - 4s_w^2 P_R) u(p_4) u(p_1) (p_1; p_2) v(p_2) \quad (A.27)$$

where $k = p_1 + p_2$, $\frac{e^2}{4} = \frac{1}{4} = 1/137.04$, $c_w = \cos \theta_w$, $s_w = \sin \theta_w$ and θ_w is the Weinberg-angle

$(p_1; p_2)$ are defined as follows:

$$(p_1; p_2) = V_{;Z}^{(1)} P_R + V_{;Z}^{(2)} P_R p_1 + V_{;Z}^{(3)} P_R p_2 +$$

$$V_{;Z}^{(4)} P_L + V_{;Z}^{(5)} P_L p_1 + V_{;Z}^{(6)} P_L p_2 \quad (A.3)$$

where $V_{;Z}^{(i)}$ are scalar function of p_1, p_2 .

R e f e r e n c e s

- [1] H.E. Haber and G.L. Kane, Phys. Rep. 117 (1985)75; J.F. Gunion and H.E. Haber, Nucl. Phys. B 272 (1986)1.
- [2] G. Farrar and P. Fayet, Phys. Lett. B 76 (1978)575
- [3] L.J. Hall and M. Suzuki, Nucl. Phys. B 231 (1984)419.
- [4] Y. Fukuda et al, Phys. Rev. Lett., 81 (1998)1562
- [5] C. Adloff et al, Z Phys. C 74 (1997)191, J. Breitweg et al, Z Phys. C 74 (1997)207, J. Butterworth and H. Dreiner, Nucl. Phys. B 397 (1993)3.
- [6] S. Weinberg, Phys. Rev. D 26 (1982)287; P. Roy, TIFR/TH/97-60; D.K. Ghosh, S. Raychaudhuri and K. Sridhar, Phys. Lett. B 396 (1997)177; K. Agashe and M. Graesser, Phys. Rev. D 54 (1996)4445; K. Huitu, J. Maalampi, M. Raidl and A. Santamaria, Phys. Lett. B 430 (1998)355; J-H. Jiang, J.G. Kim and J.S. Lee, Phys. Rev. D 55 (1997)7296; Phys. Lett. B 408 (1997)367; Phys. Rev. D 58 (1998)035006, G. Bhattacharyya, D. Choudhury and K. Sridhar, Phys. Lett. B 355 (1995)193.
- [7] R. Barbier et al, hep-ph/9810232
- [8] M. Chemtob and G. Moreau, hep-ph/9806494

- [9] C D .Froggatt and H B .N ielsen, Nucl Phys. B 147 (1979)277
- [10] D Choudhury, Phys.Lett.B 376 (1996)201.D K .G hosh et al in Ref [6]; J K alinow ski,
R Rueckl, H Spiesberger and P M .Zerwas, Phys.Lett.B 414 (1997)297, D Choudary
and S Raychaudhuri, hep-ph/9807373.
- [11] C S .Huang et al.Phys.Lett.B 452 (1999)143;
- [12] D .Atwood et al.Phys.Rev.D 53 (1996)1199; W -S.Hou and G -L.Lin, Phys.Lett.
B 379 (1996)261; Y .Jiang, M -L.Zhou, W -G .M a, L.H an, H .Zhou and M .H an, Phys.
Rev.D 57 (1998)4343.
- [13] S D im opoulos, G F G iudice and N Tetradis, NuclPhysB 454 (1995)59
- [14] R .H em p ing, Nucl.Phys.B 478 (1996)3; B .M ukhopadhy and S .R oy, Phys.Rev.
D 55 (1997)7020.
- [15] S D im opoulos and L J .H all, PhysLett.B 207 (1987)210, V B arger,G F G iudice and
T H an, PhysRevD 40 (1989)2987.
- [16] S .Bar-Shalom , G .E ilam and A .Soni, hep-ph/981251
- [17] Z-H .Yu, H P ietshm ann, W -G M a, L H an and Y J iang, hep-ph/9903471
- [18] Bernd A .K niehl, Phys.Rep. 240 (1994)211.
- [19] G .Passarino and M .Veltm an, Nucl.Phys.B 160 (1979)151.

Figure Captions

Fig.1 Feynman diagrams of $e^+e^- \rightarrow tc$ Fig.1 a: Tree-level diagrams from $L_{\tilde{\chi}_p^0}$. Fig.1 b: one-loop diagrams from $L_{\tilde{\chi}_p^0}$, dashed lines represent sleptons and squarks.

Fig.2 Cross section of $e^+e^- \rightarrow tc + ct$ as function of cm energy \sqrt{s} with $\theta_{12j}^0 = \theta_{13j}^0 = 0.01$ solid line for $m_{\tilde{t}} = m_{\tilde{q}} = 100$ GeV, and dashed line for $m_{\tilde{t}} = m_{\tilde{q}} = 150$ GeV.

Fig.3 Cross section of $e^+e^- \rightarrow tc + ct$ as function of cm energy \sqrt{s} with $\theta_{22j}^0 = 0.18$ and $\theta_{23j}^0 = 0.36$, see Ref.[5].

Fig.4 Cross section of $e^+e^- \rightarrow tc + ct$ as function of cm energy \sqrt{s} with $\theta_{323}^0 = \theta_{223}^0 = 0.625$ solid line for $m_{\tilde{t}} = m_{\tilde{q}} = 100$ GeV, and dashed line for $m_{\tilde{t}} = m_{\tilde{q}} = 150$ GeV.

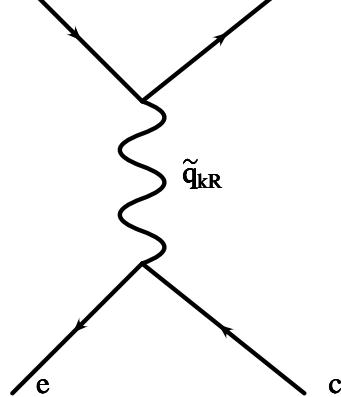


Fig 1.a

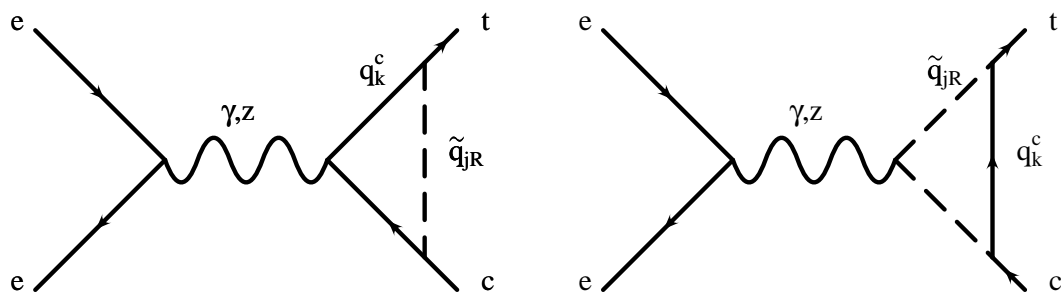
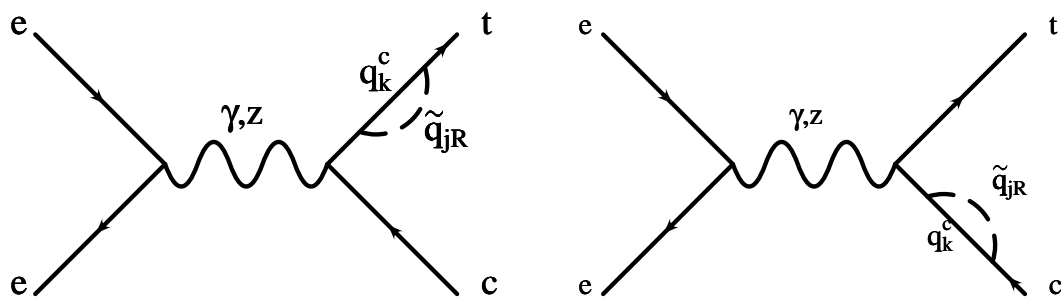


Fig 1.b

Fig.2

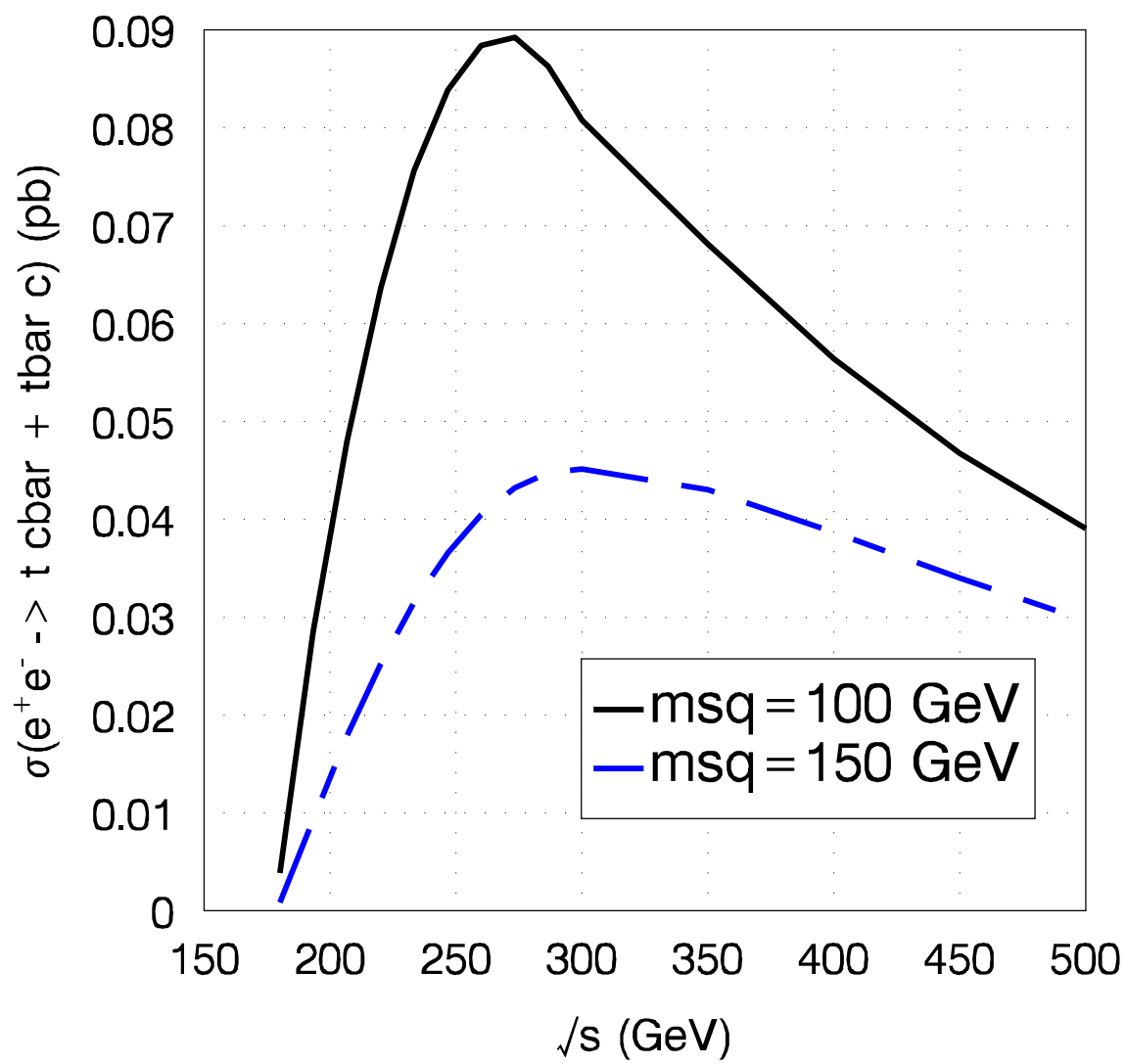


Fig.3

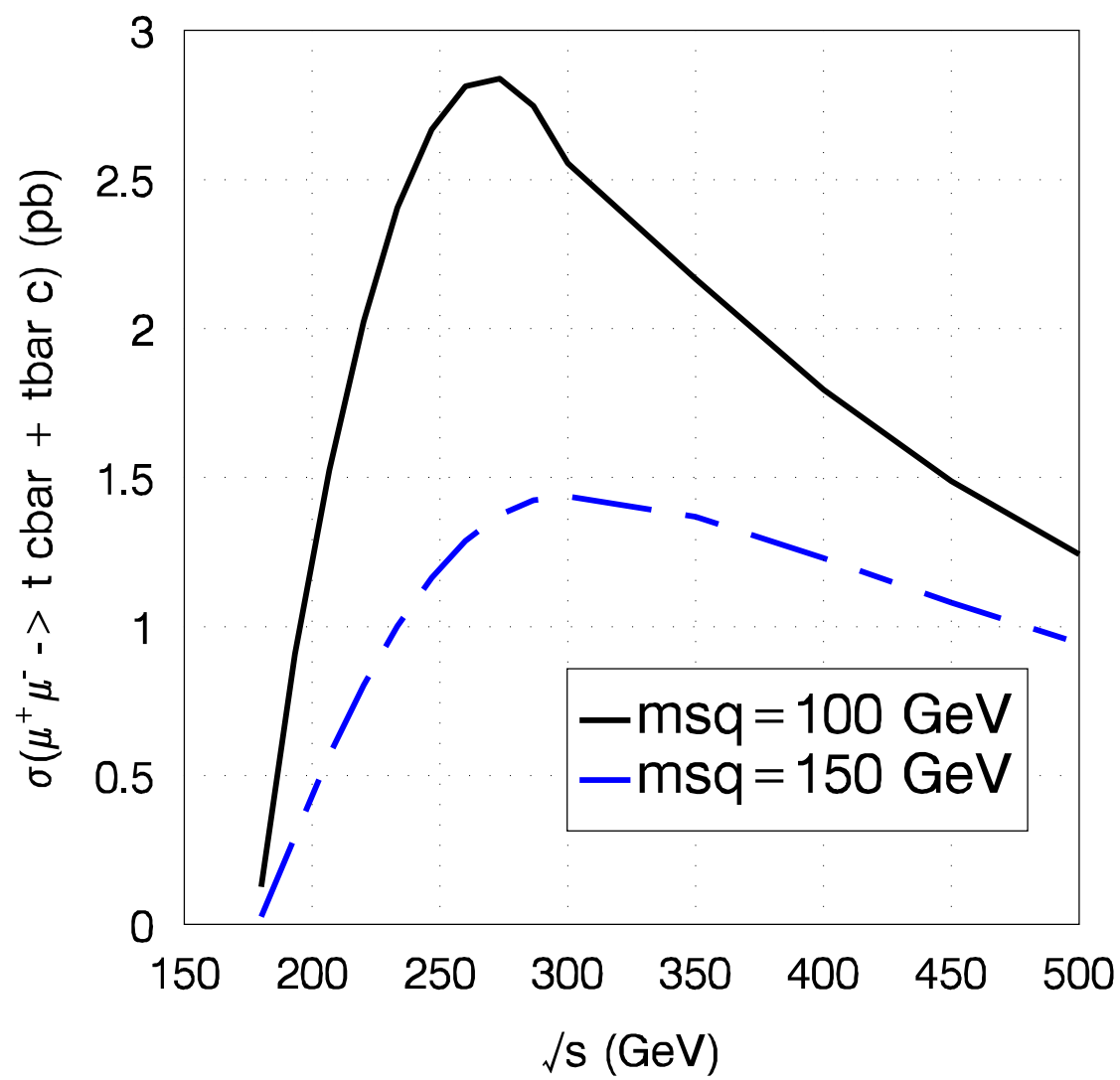


Fig.4

